

Distributed Energy and Resource Management for Full-Duplex Dense Small Cells for 5G

Animesh Yadav, Octavia A. Dobre and Nirwan Ansari*

Faculty of Engineering and Applied Science, Memorial University, St. John's, NL, Canada

*Dept. of Electrical and Computer Engineering, New Jersey Institute of Technology, Newark, NJ, USA

Email: {animeshy, odobre}@mun.ca, nirwan.ansari@njit.edu

Abstract—We consider a multi-carrier and densely deployed small cell network, where small cells are powered by renewable energy source and operate in a full-duplex mode. We formulate an energy and traffic aware resource allocation optimization problem, where a joint design of the beamformers, power and sub-carrier allocation, and users scheduling is proposed. The problem minimizes the sum data buffer lengths of each user in the network by using the harvested energy. A practical uplink user rate-dependent decoding energy consumption is included in the total energy consumption at the small cell base stations. Hence, harvested energy is shared with both downlink and uplink users. Owing to the non-convexity of the problem, a faster convergence sub-optimal algorithm based on successive parametric convex approximation framework is proposed. The algorithm is implemented in a distributed fashion, by using the alternating direction method of multipliers, which offers not only the limited information exchange between the base stations, but also fast convergence. Numerical results advocate the redesigning of the resource allocation strategy when the energy at the base station is shared among the downlink and uplink transmissions.

Index Terms—5G, small cells, full-duplex communications, energy harvesting communications, successive parametric convex approximation, radio resource management, decoding energy.

I. INTRODUCTION

For the year 2020 and beyond, the fifth generation (5G) mobile communications technology has promised to provide a 1000-fold increase in data rate and enhanced user experience. Among the technologies that have the potential to achieve the 5G promises are the dense deployment of small cells [1] and full-duplex (FD) communications. Small cells are energy- and cost-efficient base stations (BSs) that bring the users closer to them, and thus, increase the network throughput and user experience. On the other hand, the FD technique is rekindled to utilize the spectrum efficiently. The FD communications essentially allows the simultaneous transmission and reception of signals on the same time-frequency resource, and thus, improves the spectral efficiency of the network. The benefit of using the two technologies simultaneously is evident, but with a few challenges.

In a densely and arbitrarily deployed network scenario, the incumbent operators might face difficulties in powering the small cell base stations (SBSs) through the grid power source. Hence, alternately, they can install energy harvested device to each SBS for harvesting the energy from nature [2], [3]. This approach is not only environment-friendly by curbing the CO₂ emission, but also economical. Renewable energy can be freely harvested from nature using solar and wind sources. The amount and arrival of harvested energy are random by

nature, thus sometimes leading to service interruption. Hence, to reap the benefits of the freely available energy, the harvested energy must be used intelligently. With this objective, the communication system is designed with consideration of an intermittent source of energy [4]–[8].

Owing to the hardware incapability to handle self-interference (SI), the FD technique, though conceptualized a long time ago, has not been used. Recently, efforts have been made to cancel SI in both analog and digital domains jointly, e.g., [9], [10], such that FD communications become a reality. However, these works advocate the applicability of FD communications for short range, where the transmit power is low. Hence, the SBSs are the suitable candidates to operate in the FD mode [11], [12]. Furthermore, since small cells have a range of operation of approximately 100 meters, the energy spent in decoding the received data is non-negligible [13]. Hence, the SBS has to share the available energy not only with the transmitter but also with the receiver operations.

To reap the benefits of simultaneously using the energy harvesting (EH) SBS and FD communications, engineers face a few challenges: i) mitigation of interference surge due to FD communications and ii) efficient sharing of harvested energy among the transceiver operations, such as transmitting energy and rate-dependent decoding energy. At the network level, the interference intensity is high when compared with single cell scenario, due to both intra- and inter-cell interference. A few works [12], [14] studied the increase of inter-cell interference when the BS in each cell is deployed with an FD transceiver. Furthermore, the energy availability at the SBS is random and needs to be shared among the transmitter and receiver operations optimally. Hence, recent works [5], [6], [15], [16] accounted for the received data rate-dependent decoding energy (DE) in their problems for a more realistic formulation. DE is required to process the received data that are protected by some outer code, such as turbo or low-density parity check codes.

In this paper, we consider the realistic communication scenario, where densely deployed EH SBSs, operating in the FD mode, serve half-duplex (HD) downlink (DL) and uplink (UL) user equipments (UEs). The practical rate-dependent decoding power usage is included in the total power consumption at the SBSs [15], and hence, the achievable rates obtained by UL UEs are not only dependent on the UEs power, but also on that of the SBS. As a consequence, the solutions obtained in all previous works are not anymore applicable. Furthermore, to avoid the excessive resource allocations, also aligned with operators interest, we assume another realistic

assumption of non-uniform wireless traffic, i.e., each UE has different amount of data in its buffer to be transmitted. Thus, with the goal of efficiently managing the network resources in an excessive surge of interference due to FD communications and under the random energy availability, we formulate the problem of jointly designing the transmit beamformer, power and sub-carrier allocation, and UEs scheduling. Moreover, distributively solving the optimization problem is of utmost important, especially for a dense network, which requires huge information exchange among the BSs. The centralized and dual decomposition based distributed algorithms to solve the problem are discussed in [16]. Since the dual decomposition approach suffers from slow convergence, we propose to use a fast convergent alternating direction method of multipliers (ADMM) [17] approach. In this approach, we decompose the problem into SBS sub-problems by introducing the set of global variables that link the same variables of the coupled SBSs, i.e., the consensus equality constraints.

The rest of the paper is organized as follows. Section II introduces the system model and formulates the optimization problem. Section III develops an algorithm based on the ADMM framework to distributively solve the optimization problem. Section IV presents numerical results and discussions. Finally, conclusion of the paper is given in Section V.

II. SYSTEM MODEL AND PROBLEM FORMULATION

A. System Model

A multi-carrier multi-cell network consisting of B EH FD SBSs serving HD UEs is considered in [16]. Each SBS is installed with a rechargeable battery and an EH device, which are used to store and collect the harvested energy, respectively. The SBSs are equipped with $M_T + M_R$ antennas, of which M_T antennas are used to transmit data on the DL channel and M_R antennas are used to receive data on the UL channel. Each base station b belongs to a set denoted by $\mathcal{B} = \{1, \dots, B\}$. The sets of all DL and UL UEs are denoted by $\mathcal{D} = \{1, \dots, K_D\}$ and $\mathcal{U} = \{1, \dots, K_U\}$, respectively. We assume that data for the DL UE i are transmitted only from one SBS, and are denoted by $b_i \in \mathcal{B}$. Similarly, the data of UL UE j are processed by only one SBS, and are denoted by $b_j \in \mathcal{B}$. The sets of all DL and UL UEs associated with SBS b are denoted by $\mathcal{D}_b \in \mathcal{D}$ and $\mathcal{U}_b \in \mathcal{U}$, respectively. The SBSs send and receive data simultaneously to K_D UEs on the DL channels and from K_U UEs on the UL channels, respectively. We further assume that the macro base station (MBS) is serving the UEs on the UL channels. A total of N equal bandwidth sub-channels belonging to the set $\mathcal{N} = \{1, \dots, N\}$ are available in the system.

The received signal over sub-channel n at DL UE i is given by

$$\begin{aligned} \mathbf{y}_{i,n}^D &= \mathbf{h}_{b_i,i,n}^H \mathbf{u}_{i,n} s_{i,n}^D + \underbrace{\sum_{k \neq i} \mathbf{h}_{b_k,i,n}^H \mathbf{u}_{k,n} s_{k,n}^D}_{\text{MUI + CCI due to all DL UEs}} \\ &+ \underbrace{\sum_{j=1}^{K_U} g_{j,i,n} \sqrt{p_{j,n}} s_{j,n}^U + n_{i,n}^D}_{\text{CCI due to all UL UEs}}, \end{aligned} \quad (1)$$

where $\mathbf{u}_{i,n}$ and $p_{j,n}$ are the beamforming vector and power coefficient corresponding to the DL and UL UEs i and j , respectively, on the n th sub-channel. $\mathbf{h}_{b_i,i,n} \in \mathbb{C}^{M_T \times 1}$ is the channel vector from SBS b_i to DL UE i and $g_{j,i,n}$ is the complex channel coefficient from UL UE j to DL UE i on the sub-channel n . $s_{i,n}^D$ and $s_{j,n}^U$ are data symbols corresponding to the DL and UL UEs, respectively, each with unit average energy, i.e., $\mathbb{E}\{|s_{i,n}^D|^2\} = 1$. $\mathbb{E}\{\cdot\}$ denotes the expectation operator. The term $n_{i,n}^D \sim \mathcal{CN}(0, \sigma_n^2)$ is the additive white Gaussian noise (AWGN). In (1), the first and second terms on the right-hand side represent the intended signal and the sum of intra-cell multiuser interference (MUI) and inter-cell co-channel interference (CCI) due to all DL transmissions, respectively. The third term represents the CCI due to all UL transmissions. The received signal-to-interference plus noise ratio (SINR) of DL UE i over sub-channel n can be written as

$$\gamma_{i,n}^D = \frac{\mathbf{h}_{b_i,i,n}^H \mathbf{U}_{i,n} \mathbf{h}_{b_i,i,n}}{\sigma_n^2 + \sum_{k \neq i} \mathbf{h}_{b_k,i,n}^H \mathbf{U}_{k,n} \mathbf{h}_{b_k,i,n} + \sum_{j=1}^{K_U} p_{j,n} |g_{j,i,n}|^2}, \quad (2)$$

where $\mathbf{U}_{i,n} = \mathbf{u}_{i,n} \mathbf{u}_{i,n}^H$ is a positive semi-definite (PSD) matrix.

Next, for the UL transmission, the received signal vector of UE j over sub-channel n at BS b_j is given by

$$\begin{aligned} \mathbf{y}_{j,n}^U &= \mathbf{h}_{b_j,j,n} \sqrt{p_{j,n}} s_{j,n}^U + \sum_{l \neq j} \mathbf{h}_{b_j,l,n} \sqrt{p_{l,n}} s_{l,n}^U \\ &+ \underbrace{\sum_{i=1}^{K_D} \mathbf{H}_{b_j,b_i,n} \mathbf{u}_{i,n} s_{i,n}^D + \mathbf{n}_{j,n}^U}_{\text{SI + CCI from all DL UEs}}, \end{aligned} \quad (3)$$

where $\mathbf{h}_{b_j,j,n} \in \mathbb{C}^{M_R \times 1}$ is the channel vector from UL UE j to SBS b_j and $\mathbf{n}_{j,n}^U \sim \mathcal{CN}(0, \sigma_n^2 \mathbf{I}_{M_R})$ is the AWGN noise vector. In (3), the first right-hand side term is the intended signal. The second right-hand side term represents the intra-cell multiple access interference and inter-cell CCI due to all UL transmissions. The third term represents the total CCI due to inter-cell DL transmissions including SI, where $\mathbf{H}_{b_j,b_i,n}$ is the channel matrix from SBS b_j to SBS b_i . In order to recover each UL UE data, we treat the SI and CCI as background noise and apply the minimum mean square error (MMSE) successive interference cancellation receiver. Then, the received SINR of UL UE j over sub-channel n is given by

$$\begin{aligned} \gamma_{j,n}^U &= p_{j,n} \mathbf{h}_{b_j,j,n}^H \left(\sigma_n^2 \mathbf{I}_{M_R} + \sum_{l>j}^{K_U} p_{l,n} \mathbf{h}_{b_j,l,n} \mathbf{h}_{b_j,l,n}^H \right. \\ &\left. + \sum_{i=1}^{K_D} \mathbf{H}_{b_j,b_i,n} \mathbf{U}_{i,n} \mathbf{H}_{b_j,b_i,n}^H \right)^{-1} \mathbf{h}_{b_j,j,n}. \end{aligned} \quad (4)$$

We denote the number of backlogged bits waiting in the data buffer of DL UE i at the given scheduling instant by Q_i^D . At that instant, the reduction in backlogged bits achieved by the i th UE is expressed as

$$q_i^D = Q_i^D - \sum_{n=1}^N \log_2(1 + \gamma_{i,n}^D), \quad (5)$$

where the second right-hand side term is the transmission rate achieved by DL UE i . Similarly, on the UL channel, the reduction in backlogged bits achieved by the UL UE j is given by

$$q_j^{\text{U}} = Q_j^{\text{U}} - \sum_{n=1}^N \log_2(1 + \gamma_{j,n}^{\text{U}}), \quad (6)$$

where Q_j^{U} denotes the number of backlogged bits corresponding to UL UE j and the second right-hand side term represents the number of transmitted bits by UL UE j .

B. Energy Arrival and Usage Model

We consider a generic renewable energy source, at each SBS, such that the analysis presented in the sequel is valid for any energy arrival process. Let B_{\max} denote the maximum size of the rechargeable battery, which is used to store the sum of the energy harvested, i.e., $P_{b,H}$ and the leftover energy $P_{b,B}$ over the current and from the previous scheduling periods, respectively. Furthermore, at the beginning of the next scheduling period, the exact amount of energy available in the battery is known at the SBS. Hence, for a given scheduling period, the energy available at the SBS b is given as $TP_b = \min\{B_{\max}, TP_{b,H} + TP_{b,B}\}$, where T is the length of a scheduling period in seconds and the $\min(\cdot, \cdot)$ operator ensures the constraint on the maximum battery size.

In short-distance communications, the energies consumed in the circuit and decoding become comparable or even dominate the actual transmit power [13]. Hence, it is important to include them into the total power consumption, especially when the energy comes from a renewable source. The total power consumption at an SBS is expressed as:

$$P_{\text{tot},b} = \sum_{n=1}^N \sum_{i \in \mathcal{D}_b} \text{tr}(\mathbf{U}_{i,n}) + P_b^{\text{cir}} + \sum_{n=1}^N \sum_{j \in \mathcal{U}_b} P_{j,n}^{\text{dec}}(R_{j,n}), \quad (7)$$

where $P_b^{\text{cir}} = M_T P_{\text{rf}} + P_{\text{st}}$ is the total circuit power consumption, in which P_{rf} and P_{st} correspond to the active radio frequency blocks, and to the cooling and power supply, respectively. $P_{j,n}^{\text{dec}}$ is the power consumption for decoding UL UE j in sub-carrier n , where $R_{j,n} = \log_2(1 + \gamma_{j,n}^{\text{U}})$ is the achievable rate of the UE. Note that the decoding power consumption is a function of the data rate of the UE: for example, for an UL UE j , $P_{j,n}^{\text{dec}}(R_{j,n}) = \alpha_j R_{j,n}$ where α_j models the decoder efficiency, being decoder specific [13], [15].

C. Optimization Problem Formulation

In this work, we are interested in reducing the total number of backlogged bits in the network by minimizing the ℓ_2 -norm of the deviation metrics given in (5) and (6) [16]. The main reason for using the ℓ_2 -norm in the objective function is that it gives priority to the UE with a large queued data in the buffer.

Now, by denoting $\mathbf{U} = [\mathbf{U}_1, \dots, \mathbf{U}_B]$, where $\mathbf{U}_b = [\mathbf{U}_{\mathcal{D}_b(1),1}, \dots, \mathbf{U}_{\mathcal{D}_b(|\mathcal{D}_b|),N}]^1$ and $\mathbf{p} = [\mathbf{p}_1, \dots, \mathbf{p}_B]$, where $\mathbf{p}_b = [p_{\mathcal{U}_b(1),1}, \dots, p_{\mathcal{U}_b(|\mathcal{U}_b|),N}]$, the optimization problem

¹ $\mathcal{A}(i)$ and $|\mathcal{A}|$ denote the i th element and cardinality of set \mathcal{A} , respectively.

to be solved at the beginning of each scheduling period is formulated as

$$\min_{\mathbf{U}, \mathbf{p}} \|\mathbf{q}_{\text{D}}\|_2 + \|\mathbf{q}_{\text{U}}\|_2 \quad (8a)$$

$$\text{s.t.} \sum_{n=1}^N \sum_{i \in \mathcal{D}_b} \text{tr}(\mathbf{U}_{i,n}) \leq P_{b,\max} \quad \forall b, \quad (8b)$$

$$P_{\text{tot},b} \leq P_b \quad \forall b, \quad (8c)$$

$$\sum_{n=1}^N p_{j,n} \leq P_{u,\max} \quad \forall j \in \mathcal{U}, \quad (8d)$$

$$\text{rank}(\mathbf{U}_{i,n}) = 1 \quad \forall i \in \mathcal{D}, \forall n, \quad (8e)$$

$$\mathbf{U}_{i,n} \succeq 0 \quad \forall i \in \mathcal{D}, \forall n, \quad (8f)$$

$$p_{j,n} \geq 0 \quad \forall j \in \mathcal{U}, \forall n, \quad (8g)$$

where \mathbf{q}_{D} and \mathbf{q}_{U} have the elements q_i^{D} and q_j^{U} , respectively. $P_{b,\max}$ is the maximum total transmit power constraint on the DL channel, and $P_{u,\max}$ is the individual UE transmit power constraint on the UL channel. It is worth noting that (8)² implicitly solves the problem of sub-carrier allocation and UE scheduling as well. Hence, the optimization problem jointly designs the beamformers, power and sub-carrier allocation and UE scheduling. An UE is scheduled whenever it is allocated a non-zero power on a sub-carrier; otherwise, it is not.

In (8), the objective function (8a) ensures avoidance of the redundant resource allocation, which is limited by the data queue length of the UEs. Further, constraint (8b) ensures that the maximum transmit power allowed by SBS b for the DL transmission is limited by $P_{b,\max}$. Constraint (8c) ensures the available energy at the SBS is drawn by both the transmitter and receiver operations, and the energy causality constraint. In general, it is difficult to solve the above optimization problem due to the rank-one constraint. Hence, we relax the rank-one constraint and express the relaxed problem as

$$\underset{\mathbf{U}, \mathbf{p}}{\text{minimize}} \{ \|\mathbf{q}_{\text{D}}\|_2 + \|\mathbf{q}_{\text{U}}\|_2 \mid (8b) - (8d), (8f), (8g) \}. \quad (9)$$

Owing to the non-concave objective function and constraint (8c) in (9), we propose to solve it by using the successive parametric convex approximation (SPCA) method [18]. In this method, (9) is successively approximated to a convex problem as presented in Proposition 1, to obtain progressively improved solution.

Proposition 1: By introducing the auxiliary variables β_b , \mathbf{t}_b , \mathbf{x}_b , and \mathbf{z}_b for all $b \in \{1, \dots, B\}$, the convex approximate of (9), at the r th SPCA iteration, is expressed as

$$\min_{\underline{\mathbf{U}}} \|\tilde{\mathbf{q}}_{\text{D}}\|_2 + \|\tilde{\mathbf{q}}_{\text{U}}\|_2 \quad (10a)$$

$$\text{s.t.} \mathbf{h}_{b_i,i,n}^H \mathbf{U}_{i,n} \mathbf{h}_{b_i,i,n} \geq F(z_{i,n}^{\text{D}}, \beta_{i,n}, \xi^{[r]}) \forall i \in \mathcal{D}, \forall n, \quad (10b)$$

$$H(x_{j,n}, \mathbf{p}_{\mathcal{U} \setminus \{j\}}, \mathbf{U}, x_{j,n}^{[r]}, \mathbf{p}_{\mathcal{U} \setminus \{j\}}^{[r]}, \mathbf{U}^{[r]}) \leq z_{j,n}^{\text{U}} \quad \forall j \in \mathcal{U}, \forall n, \quad (10c)$$

$$\sum_{n=1}^N \sum_{i \in \mathcal{D}_b} \text{tr}(\mathbf{U}_{i,n}) \leq P_{b,\max} \quad \forall b, \quad (10d)$$

²Note that (8) represents equations (8a)-(8g). A similar notation is employed throughout the paper.

$$P_b^{\text{cir}} + \sum_{n=1}^N \sum_{j \in \mathcal{U}_b} \alpha_j t_{j,n}^{\text{U}} + \sum_{n=1}^N \sum_{i \in \mathcal{D}_b} \text{tr}(\mathbf{U}_{i,n}) \leq P_b \forall b, \quad (10e)$$

$$e^{t_{i,n}^{\text{D}}} \leq z_{i,n}^{\text{D}} + 1 \quad \forall i \in \mathcal{D}, \forall n, \quad (10f)$$

$$\sigma_n^2 + \sum_{k \neq i}^{K_{\mathcal{D}_b}} \mathbf{h}_{b_k,i,n}^H \mathbf{U}_{k,n} \mathbf{h}_{b_k,i,n} + \sum_{j=1}^{K_{\mathcal{U}_b}} p_{j,n} |g_{j,i,n}|^2 \leq \beta_{i,n} \quad \forall i \in \mathcal{D}, \forall n, \quad (10g)$$

$$p_{j,n} \geq x_{j,n}^2 \quad \forall j \in \mathcal{U}, \forall n, \quad (10h)$$

$$e^{t_{j,n}^{\text{U}}} \leq z_{j,n}^{\text{U}} + 1 \quad \forall j \in \mathcal{U}, \forall n, \quad (10i)$$

$$(8d), (8f), (8g), \quad (10j)$$

where $F(z_{i,n}^{\text{D}}, \beta_{i,n}, \xi^{[r]}) = \beta_{i,n}^2 / (2\xi^{[r]}) + \xi^{[r]} (z_{i,n}^{\text{D}})^2 / 2$ and $H(x_{j,n}, \mathbf{p}_{\mathcal{U} \setminus \{j\}}, \mathbf{U}, x_{j,n}^{[r]}, \mathbf{p}_{\mathcal{U} \setminus \{j\}}^{[r]}, \mathbf{U}^{[r]})$ is a convex approximate of function $x_{j,n}^2 \mathbf{h}_{b_j,j,n}^H \mathbf{X}_{j,n}^{-1} \mathbf{h}_{b_j,j,n}$ at the r th iterate, where $\mathbf{X}_{j,n} \triangleq \sigma_n^2 \mathbf{I}_{M_R} + \sum_{l>j} p_{l,n} \mathbf{h}_{b_j,l,n} \mathbf{h}_{b_j,l,n}^H + \sum_{i=1}^{K_{\mathcal{D}_b}} \mathbf{H}_{b_j,b_i,n} \mathbf{W}_{i,n} \mathbf{H}_{b_j,b_i,n}$. $\Xi = \{\Xi_1, \dots, \Xi_B\}$ and Ξ_b collects the variables corresponding to the BS b , i.e., $\{\mathbf{U}_b, \mathbf{p}_b, \beta_b, \mathbf{t}_b, \mathbf{x}_b, \mathbf{z}_b\}$, where $\beta_b = [\beta_{\mathcal{D}_b(1),1}, \dots, \beta_{\mathcal{D}_b(|\mathcal{D}_b|),N}]$, $\mathbf{t}_b = [t_{\mathcal{D}_b(1),1}^{\text{D}}, \dots, t_{\mathcal{D}_b(|\mathcal{D}_b|),N}^{\text{D}}, t_{\mathcal{U}_b(1),1}^{\text{U}}, \dots, t_{\mathcal{U}_b(|\mathcal{U}_b|),N}^{\text{U}}]$, $\mathbf{x}_b = [x_{\mathcal{U}_b(1),1}, \dots, x_{\mathcal{U}_b(|\mathcal{U}_b|),N}]$, and $\mathbf{z}_b = [z_{\mathcal{D}_b(1),1}^{\text{D}}, \dots, z_{\mathcal{D}_b(|\mathcal{D}_b|),N}^{\text{D}}, z_{\mathcal{U}_b(1),1}^{\text{U}}, \dots, z_{\mathcal{U}_b(|\mathcal{U}_b|),N}^{\text{U}}]$. The superscript $[r]$ denotes the value of the scripted variable at the r th iteration.

Proof: The proof is based on the description given in [16, Sec. III]. \blacksquare

Using Proposition 1, (9) can be solved in a centralized fashion [16] at the cost of heavy information exchange.

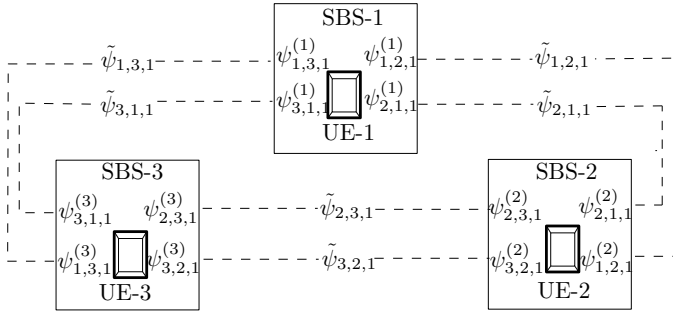


Fig. 1. Three small cells network each with one DL UE. $\mathcal{B} = \{1, 2, 3\}$, $\mathcal{D}_1 = \{2, 3\}$, $\mathcal{D}_2 = \{1, 3\}$, $\mathcal{D}_3 = \{1, 2\}$.

III. DISTRIBUTED SOLUTION

Owing to the FD communications, twice the amount of information exchange is required as compared to the HD counterpart for solving the problem in a centralized manner. Furthermore, for a dense network, information exchange requires extra resources that decrease the spectral efficiency of the network. Hence, turning to a distributed approach, where each SBS independently designs the beamformers and power allocations locally with minimal information exchange with the rest of the SBSs, is a necessity.

In order to implement a distributed approach, we take advantage of the separability of the objective function with

respect to (w.r.t.) each BS, and hence (10) can be written equivalently as

$$\min_{\Xi} \left\{ \sum_{b \in \mathcal{B}} \|\tilde{\mathbf{q}}_{b,b}\|_2 + \sum_{b \in \mathcal{B}} \|\tilde{\mathbf{q}}_{b,b}\|_2 \mid (10b) - (10j) \right\}, \quad (11)$$

where $\tilde{\mathbf{q}}_{\mathcal{D},b}$ and $\tilde{\mathbf{q}}_{\mathcal{U},b}$ denote the queue deviations of the DL and UL UEs associated with b , respectively. Observe that the constraints in (11) are not separable; in particular, constraints (10c) and (10g) are coupled through the inter-cell CCI terms. To this end, we rewrite (11) as

$$\min_{\Xi} \sum_{b \in \mathcal{B}} \|\tilde{\mathbf{q}}_{b,b}\|_2 + \sum_{b \in \mathcal{B}} \|\tilde{\mathbf{q}}_{b,b}\|_2 \quad (12a)$$

$$\text{s.t. } \sigma_n^2 + \sum_{k \in \mathcal{D}_b \setminus \{i\}} \mathbf{h}_{b_k,i,n}^H \mathbf{U}_{k,n} \mathbf{h}_{b_k,i,n} + \sum_{\bar{b} \in \bar{\mathcal{B}}_b} \psi_{\bar{b},i,n}^{(b)} + \sum_{j \in \mathcal{U}_b} p_{j,n} |g_{j,i,n}|^2 + \sum_{\bar{b} \in \bar{\mathcal{B}}_b} \phi_{\bar{b},i,n}^{(b)} \leq \beta_{i,n} \quad \forall i \in \mathcal{D}, \forall n, \quad (12b)$$

$$\psi_{b,i,n}^{(b)} \geq \sum_{k \in \mathcal{D}_b} \mathbf{h}_{b,i,n}^H \mathbf{U}_{k,n} \mathbf{h}_{b,i,n} \quad \forall b, \forall i \in \bar{\mathcal{D}}_b, \forall n, \quad (12c)$$

$$\phi_{b,i,n}^{(b)} \geq \sum_{l \in \mathcal{U}_b} p_{l,n} |g_{l,i,n}|^2 \quad \forall b, \forall i \in \bar{\mathcal{D}}_b, \forall n, \quad (12d)$$

$$\Psi_{b,j,n}^{(b)} \succeq \sum_{l \in \mathcal{U}_b} p_{l,n} \mathbf{h}_{b_j,l,n} \mathbf{h}_{b_j,l,n}^H \quad \forall b, \forall j \in \bar{\mathcal{U}}_b, \forall n, \quad (12e)$$

$$\Phi_{b,j,n}^{(b)} \succeq \sum_{i \in \mathcal{D}_b} \mathbf{H}_{b,b_j,n} \mathbf{U}_{i,n} \mathbf{H}_{b,b_j,n}^H \quad \forall b, \forall j \in \bar{\mathcal{U}}_b, \forall n, \quad (12f)$$

$$\psi_{b,i,n}^{(b)} = \tilde{\psi}_{b,i,n} \quad \forall b, \forall i \in \bar{\mathcal{D}}_b, \forall n, \quad (12g)$$

$$\psi_{\bar{b},i,n}^{(b)} = \tilde{\psi}_{\bar{b},i,n} \quad \forall b, \forall \bar{b} \in \bar{\mathcal{B}}_b, \forall i \in \mathcal{D}_b, \forall n, \quad (12h)$$

$$\phi_{b,i,n}^{(b)} = \tilde{\phi}_{b,i,n} \quad \forall b, \forall i \in \bar{\mathcal{D}}_b, \forall n, \quad (12i)$$

$$\phi_{\bar{b},i,n}^{(b)} = \tilde{\phi}_{\bar{b},i,n} \quad \forall b, \forall \bar{b} \in \bar{\mathcal{B}}_b, \forall i \in \mathcal{D}_b, \forall n, \quad (12j)$$

$$\Psi_{b,j,n}^{(b)} = \tilde{\Psi}_{b,j,n} \quad \forall b, \forall j \in \bar{\mathcal{U}}_b, \forall n, \quad (12k)$$

$$\Psi_{\bar{b},j,n}^{(b)} = \tilde{\Psi}_{\bar{b},j,n} \quad \forall b, \forall \bar{b} \in \bar{\mathcal{B}}_b, \forall j \in \mathcal{U}_b, \forall n, \quad (12l)$$

$$\Phi_{b,j,n}^{(b)} = \tilde{\Phi}_{b,j,n} \quad \forall b, \forall j \in \bar{\mathcal{U}}_b, \forall n, \quad (12m)$$

$$\Phi_{\bar{b},j,n}^{(b)} = \tilde{\Phi}_{\bar{b},j,n} \quad \forall b, \forall \bar{b} \in \bar{\mathcal{B}}_b, \forall j \in \mathcal{U}_b, \forall n, \quad (12n)$$

$$(10b) - (10f), (10h) - (10j), \quad (12o)$$

where $\bar{\mathcal{B}}_b$, $\bar{\mathcal{D}}_b$ and $\bar{\mathcal{U}}_b$ denote the sets $\mathcal{B} \setminus \{b\}$, $\mathcal{D} \setminus \{\mathcal{D}_b\}$ and $\mathcal{U} \setminus \{\mathcal{U}_b\}$, respectively. $\psi_{b,i,n}$ and $\phi_{b,i,n}$ are newly introduced auxiliary variables, respectively, representing the inter-cell CCI caused by the DL and UL transmissions of BS b to the neighboring cells DL UE $i \in \bar{\mathcal{D}}_b$. Similarly, $\Psi_{b,j,n}$ and $\Phi_{b,j,n}$ are newly introduced auxiliary variables, respectively, representing the inter-cell CCI covariance matrices caused by the UL and DL transmissions of the BS b to the neighboring cells UL UE $j \in \bar{\mathcal{U}}_b$. The superscript (\cdot) denotes the local copy of the variable. To simplify the decoupling, equality constraints (12g)-(12m) are introduced, where $\tilde{\phi}_{b,i,n}$, $\tilde{\psi}_{b,i,n}$, $\tilde{\Phi}_{b,i,n}$, and $\tilde{\Psi}_{b,i,n} \forall b, \forall i \in \bar{\mathcal{D}}_b, \forall n$ are the global variables. Each global variable links the two local variables of the coupled BSs. For instance, consider a three SBS network scenario, as depicted in Fig. 1, for $b = 1$, $\tilde{\phi}_{1,2,1}$ represents the same variables $\phi_{1,2,1}^{(1)}$ and $\phi_{1,2,1}^{(2)}$ corresponding to the BS $b = 1$ and $b = 2$, respectively, and so on for all other coupling variables. The equivalence between (11) and (12) is due to the fact that constraints (12b)-(12f) hold with equality at optimality.

Observe that (12) is in a suitable form to apply distributed optimization. The dual decomposition [17] framework offers distributed implementation; however, it suffers from slow convergence. Here, we prefer to use a fast convergence implementation using the ADMM [17] framework. For that, we first write the partial augmented Lagrangian dual of (12) w.r.t. the equality constraints as

$$\begin{aligned}
\mathcal{L}(\Xi, \mathcal{X}, \tilde{\mathcal{X}}, \hat{\mathcal{X}}) &= \sum_{b \in \mathcal{B}} \|\tilde{\mathbf{q}}_{D,b}\|_2 + \sum_{b \in \mathcal{B}} \|\tilde{\mathbf{q}}_{U,b}\|_2 \\
&+ \sum_{b \in \mathcal{B}_b} \sum_{n=1}^N \left[\sum_{i \in \bar{\mathcal{D}}_b} \theta_{b,i,n} (\psi_{b,i,n}^{(b)} - \tilde{\psi}_{b,i,n}) + \frac{\rho_1}{2} (\psi_{b,i,n}^{(b)} - \tilde{\psi}_{b,i,n})^2 \right. \\
&+ \sum_{\bar{b} \in \bar{\mathcal{B}}_b} \sum_{i \in \mathcal{D}_b} \theta_{\bar{b},i,n} (\psi_{\bar{b},i,n}^{(b)} - \tilde{\psi}_{\bar{b},i,n}) + \frac{\rho_1}{2} (\psi_{\bar{b},i,n}^{(b)} - \tilde{\psi}_{\bar{b},i,n})^2 \\
&+ \sum_{i \in \bar{\mathcal{D}}_b} \omega_{b,i,n} (\phi_{b,i,n}^{(b)} - \tilde{\phi}_{b,i,n}) + \frac{\rho_2}{2} (\phi_{b,i,n}^{(b)} - \tilde{\phi}_{b,i,n})^2 \\
&+ \sum_{\bar{b} \in \bar{\mathcal{B}}_b} \sum_{i \in \mathcal{D}_b} \omega_{\bar{b},i,n} (\phi_{\bar{b},i,n}^{(b)} - \tilde{\phi}_{\bar{b},i,n}) + \frac{\rho_2}{2} (\phi_{\bar{b},i,n}^{(b)} - \tilde{\phi}_{\bar{b},i,n})^2 \\
&+ \sum_{j \in \bar{\mathcal{U}}_b} \text{tr}(\Theta_{b,j,n} (\Psi_{b,j,n}^{(b)} - \tilde{\Psi}_{b,j,n})) + \frac{\rho_3}{2} \|\Psi_{b,j,n}^{(b)} - \tilde{\Psi}_{b,j,n}\|_2^2 + \\
&\sum_{\bar{b} \in \bar{\mathcal{B}}_b} \sum_{j \in \mathcal{U}_b} \text{tr}(\Theta_{\bar{b},j,n} (\Psi_{\bar{b},j,n}^{(b)} - \tilde{\Psi}_{\bar{b},j,n})) + \frac{\rho_3}{2} \|\Psi_{\bar{b},j,n}^{(b)} - \tilde{\Psi}_{\bar{b},j,n}\|_2^2 \\
&+ \sum_{j \in \bar{\mathcal{U}}_b} \text{tr}(\Omega_{b,j,n} (\Phi_{b,j,n}^{(b)} - \tilde{\Phi}_{b,j,n})) + \frac{\rho_4}{2} \|\Phi_{b,j,n}^{(b)} - \tilde{\Phi}_{b,j,n}\|_2^2 + \\
&\sum_{\bar{b} \in \bar{\mathcal{B}}_b} \sum_{j \in \mathcal{U}_b} \text{tr}(\Omega_{\bar{b},j,n} (\Phi_{\bar{b},j,n}^{(b)} - \tilde{\Phi}_{\bar{b},j,n})) + \frac{\rho_4}{2} \|\Phi_{\bar{b},j,n}^{(b)} - \tilde{\Phi}_{\bar{b},j,n}\|_2^2 \Big]
\end{aligned} \tag{13}$$

where $\rho_1, \rho_2, \rho_3,$ and ρ_4 are the positive penalty parameters that controls the rate of convergence. All the local variables are collected into $\mathcal{X} = \{\mathcal{X}_1, \dots, \mathcal{X}_B\}$, where \mathcal{X}_b collects $\{\phi^{(b)}, \psi^{(b)}, \Psi^{(b)}, \Phi^{(b)}\}$ and $\phi^{(b)}$ collects $\{\phi_{b, \bar{\mathcal{D}}_b(1), 1}, \dots, \phi_{b, \bar{\mathcal{D}}_b(|\bar{\mathcal{D}}_b|), N}, \phi_{\bar{\mathcal{B}}_b(1), \mathcal{D}_b(1), 1}, \dots, \phi_{\bar{\mathcal{B}}_b(|\bar{\mathcal{B}}_b|), \mathcal{D}_b(|\mathcal{D}_b|), N}\}$ and similarly $\psi^{(b)}, \Psi^{(b)},$ and $\Phi^{(b)}$ are represented. Similarly, all the global variables are collected into $\tilde{\mathcal{X}} = \{\tilde{\mathcal{X}}_1, \dots, \tilde{\mathcal{X}}_B\}$, where $\tilde{\mathcal{X}}_b$ collects $\{\tilde{\phi}_b, \tilde{\psi}_b, \tilde{\Psi}_b, \tilde{\Phi}_b\}$ and ϕ_b collects $\{\phi_{b, \bar{\mathcal{D}}_b(1), 1}, \dots, \phi_{b, \bar{\mathcal{D}}_b(|\bar{\mathcal{D}}_b|), N}, \phi_{\bar{\mathcal{B}}_b(1), \mathcal{D}_b(1), 1}, \dots, \phi_{\bar{\mathcal{B}}_b(|\bar{\mathcal{B}}_b|), \mathcal{D}_b(|\mathcal{D}_b|), N}\}$ and similarly $\psi, \Psi,$ and Φ are represented. Similarly, the Lagrangian multipliers are collected in $\hat{\mathcal{X}} = \{\hat{\mathcal{X}}_1, \dots, \hat{\mathcal{X}}_B\}$, where $\hat{\mathcal{X}}_b$ collects $\{\theta_b, \omega_b, \Theta_b, \Omega_b\}$ with its elements represented similarly as of the local and global variables.

Now, the independent b th sub-problem for the v th iteration is expressed as

$$\min f_b(\Xi_b, \mathcal{X}_b, \tilde{\mathcal{X}}_b^{[v]}, \hat{\mathcal{X}}_b^{[v]}) \tag{14a}$$

$$\text{s.t. } \sigma_n^2 + \sum_{k \in \mathcal{D}_b \setminus \{i\}} \mathbf{h}_{b,k,i,n}^H \mathbf{U}_{k,n} \mathbf{h}_{b,k,i,n} + \sum_{\bar{b} \in \bar{\mathcal{B}}_b} \psi_{\bar{b},i,n}^{(b)} \tag{14b}$$

$$+ \sum_{j \in \bar{\mathcal{U}}_b} p_{j,n} |g_{j,i,n}|^2 + \sum_{\bar{b} \in \bar{\mathcal{B}}_b} \phi_{\bar{b},i,n}^{(b)} \leq \beta_{i,n} \quad \forall i \in \mathcal{D}_b, \forall n, \tag{14c}$$

$$\psi_{b,i,n}^{(b)} \geq \sum_{k \in \mathcal{D}_b} \mathbf{h}_{b,i,k,n}^H \mathbf{U}_{k,n} \mathbf{h}_{b,i,n} \quad \forall i \in \bar{\mathcal{D}}_b, \tag{14d}$$

$$\phi_{b,i,n}^{(b)} \geq \sum_{l \in \mathcal{U}_b} \rho_{l,n} |g_{l,i,n}|^2 \quad \forall i \in \bar{\mathcal{D}}_b, \tag{14e}$$

$$\Psi_{b,j,n}^{(b)} \preceq \sum_{l \in \mathcal{U}_b} \rho_{l,n} \mathbf{h}_{b,j,l,n} \mathbf{h}_{b,j,l,n}^H \quad \forall j \in \bar{\mathcal{U}}_b, \tag{14f}$$

$$\Phi_{b,j,n}^{(b)} \preceq \sum_{k \in \mathcal{D}_b} \mathbf{H}_{b,b,j,n} \mathbf{U}_{k,n} \mathbf{H}_{b,b,j,n}^H \quad \forall j \in \bar{\mathcal{U}}_b, \tag{14g}$$

$$\tag{12o}, \tag{14h}$$

where $f_b(\Xi_b, \mathcal{X}_b, \tilde{\mathcal{X}}_b^{[v]}, \hat{\mathcal{X}}_b^{[v]}) = \|\tilde{\mathbf{q}}_{D,b}\|_2 + \|\tilde{\mathbf{q}}_{U,b}\|_2$

$$\begin{aligned}
&+ \sum_{n=1}^N \left[\sum_{i \in \bar{\mathcal{D}}_b} \theta_{b,i,n}^{[v]} (\psi_{b,i,n}^{(b)} - \tilde{\psi}_{b,i,n}^{[v]}) + \frac{\rho_1}{2} (\psi_{b,i,n}^{(b)} - \tilde{\psi}_{b,i,n}^{[v]})^2 \right. \\
&+ \sum_{\bar{b} \in \bar{\mathcal{B}}_b} \sum_{i \in \mathcal{D}_b} \theta_{\bar{b},i,n}^{[v]} (\psi_{\bar{b},i,n}^{(b)} - \tilde{\psi}_{\bar{b},i,n}^{[v]}) + \frac{\rho_1}{2} (\psi_{\bar{b},i,n}^{(b)} - \tilde{\psi}_{\bar{b},i,n}^{[v]})^2 \\
&+ \sum_{i \in \bar{\mathcal{D}}_b} \omega_{b,i,n}^{[v]} (\phi_{b,i,n}^{(b)} - \tilde{\phi}_{b,i,n}^{[v]}) + \frac{\rho_2}{2} (\phi_{b,i,n}^{(b)} - \tilde{\phi}_{b,i,n}^{[v]})^2 \\
&+ \sum_{\bar{b} \in \bar{\mathcal{B}}_b} \sum_{i \in \mathcal{D}_b} \omega_{\bar{b},i,n}^{[v]} (\phi_{\bar{b},i,n}^{(b)} - \tilde{\phi}_{\bar{b},i,n}^{[v]}) + \frac{\rho_2}{2} (\phi_{\bar{b},i,n}^{(b)} - \tilde{\phi}_{\bar{b},i,n}^{[v]})^2 \\
&+ \sum_{j \in \bar{\mathcal{U}}_b} \text{tr}(\Theta_{b,j,n}^{[v]} (\Psi_{b,j,n}^{(b)} - \tilde{\Psi}_{b,j,n}^{[v]})) + \frac{\rho_3}{2} \|\Psi_{b,j,n}^{(b)} - \tilde{\Psi}_{b,j,n}^{[v]}\|_2^2 + \\
&\sum_{\bar{b} \in \bar{\mathcal{B}}_b} \sum_{j \in \mathcal{U}_b} \text{tr}(\Theta_{\bar{b},j,n}^{[v]} (\Psi_{\bar{b},j,n}^{(b)} - \tilde{\Psi}_{\bar{b},j,n}^{[v]})) + \frac{\rho_3}{2} \|\Psi_{\bar{b},j,n}^{(b)} - \tilde{\Psi}_{\bar{b},j,n}^{[v]}\|_2^2 \\
&+ \sum_{j \in \bar{\mathcal{U}}_b} \text{tr}(\Omega_{b,j,n}^{[v]} (\Phi_{b,j,n}^{(b)} - \tilde{\Phi}_{b,j,n}^{[v]})) + \frac{\rho_4}{2} \|\Phi_{b,j,n}^{(b)} - \tilde{\Phi}_{b,j,n}^{[v]}\|_2^2 + \\
&\sum_{\bar{b} \in \bar{\mathcal{B}}_b} \sum_{j \in \mathcal{U}_b} \text{tr}(\Omega_{\bar{b},j,n}^{[v]} (\Phi_{\bar{b},j,n}^{(b)} - \tilde{\Phi}_{\bar{b},j,n}^{[v]})) + \frac{\rho_4}{2} \|\Phi_{\bar{b},j,n}^{(b)} - \tilde{\Phi}_{\bar{b},j,n}^{[v]}\|_2^2 \Big],
\end{aligned}$$

and $\hat{\mathcal{X}}_b^{[v]}$ and $\tilde{\mathcal{X}}_b^{[v]}$ denote the collection of fixed Lagrangian multipliers and interference variables updated from the previous iterations. The optimization variables of the problem are Ξ_b . After solving (14) for $\Xi_b, \psi^{(b)}, \phi^{(b)}, \Psi^{(b)},$ and $\Phi^{(b)} \forall b$ in the v th iteration, in the next step, the interference terms are exchanged between BSs b and b_i as

$$\tilde{\psi}_{b,i,n}^{[v+1]} = 0.5(\psi_{b,i,n}^{(b)} + \psi_{b,i,n}^{(b_i)}) \quad \forall b, \forall i \in \bar{\mathcal{D}}_b, \forall n, \tag{15}$$

$$\tilde{\phi}_{b,i,n}^{[v+1]} = 0.5(\phi_{b,i,n}^{(b)} + \phi_{b,i,n}^{(b_i)}) \quad \forall b, \forall i \in \bar{\mathcal{D}}_b, \forall n, \tag{16}$$

$$\tilde{\Psi}_{b,j,n}^{[v+1]} = 0.5(\Psi_{b,j,n}^{(b)} + \Psi_{b,j,n}^{(b_j)}) \quad \forall b, \forall j \in \bar{\mathcal{U}}_b, \forall n, \tag{17}$$

$$\tilde{\Phi}_{b,j,n}^{[v+1]} = 0.5(\Phi_{b,j,n}^{(b)} + \Phi_{b,j,n}^{(b_j)}) \quad \forall b, \forall j \in \bar{\mathcal{U}}_b, \forall n. \tag{18}$$

The final step of the ADMM approach is the Lagrangian multipliers update, which is given as

$$\theta_{b,i,n}^{[v+1]} = [\theta_{b,i,n}^{[v]} + \rho_1^{[v]} (\psi_{b,i,n}^{(b)} - \tilde{\psi}_{b,i,n}^{[v+1]})] \quad \forall b, \forall i, \forall n, \tag{19}$$

$$\omega_{b,i,n}^{[v+1]} = [\omega_{b,i,n}^{[v]} + \rho_2^{[v]} (\phi_{b,i,n}^{(b)} - \tilde{\phi}_{b,i,n}^{[v+1]})] \quad \forall b, \forall i, \forall n, \tag{20}$$

$$\Theta_{b,j,n}^{[v+1]} = [\Theta_{b,j,n}^{[v]} + \rho_3^{[v]} (\Psi_{b,j,n}^{(b)} - \tilde{\Psi}_{b,j,n}^{[v+1]})^T] \quad \forall b, \forall j, \forall n, \tag{21}$$

$$\Omega_{b,j,n}^{[v+1]} = [\Omega_{b,j,n}^{[v]} + \rho_4^{[v]} (\Phi_{b,j,n}^{(b)} - \tilde{\Phi}_{b,j,n}^{[v+1]})^T] \quad \forall b, \forall j, \forall n. \tag{22}$$

Now, in the r th SPCA iteration index, after the convergence of the ADMM procedure, the optimization variables in the set Ξ are updated until the convergence of the SPCA procedure. The pseudo code of the ADMM based distributed algorithm is summarized in Algorithm 1.

Algorithm 1 ADMM based distributed iterative algorithm

Input: $\mathbf{h}, \mathbf{g}, \sigma_n, P_b^{\text{cir}}, P_{b,\text{max}}, P_b, P_{u,\text{max}}, \alpha, I_{\text{max},1}, I_{\text{max},2}$.

Output: \mathbf{U}, \mathbf{p} .

- 1: Initialize $r := 0; v := 0, \Xi^{[0]}, \tilde{\mathcal{X}}^{[0]}$, and $\hat{\mathcal{X}}^{[0]} = 0$;
 - 2: **repeat**
 - 3: **repeat**
 - 4: Solve (14) for $\Xi_b^{[r]}, \mathcal{X}_b^{[v]}, \tilde{\mathcal{X}}_b^{[v]} \forall b \in \mathcal{B}$ using $\hat{\mathcal{X}}_b^{[v]}$
 - 5: Exchange $\mathcal{X}_b^{[v]}$ among BSs
 - 6: Update $\tilde{\mathcal{X}}_b^{[v+1]}$ using (15) – (18)
 - 7: Update $\hat{\mathcal{X}}_b^{[v+1]}$ using (19) – (22)
 - 8: Set $v := v + 1$
 - 9: **until** Convergence of ADMM algo. or $v \geq I_{\text{max},2}$
 - 10: Update $\Xi^{[r+1]} = \Xi^*$;
 - 11: $r := r + 1; v := 0$
 - 12: **until** Queue convergence or $r \geq I_{\text{max},1}$
 - 13: Perform randomization to extract a rank-one solution
-

 TABLE I
 SIMULATION PARAMETERS

Parameters	Value
No. of antennas	$M_T = 2, M_R = 2$
No. of sub-carriers	$N = 2$
Cell radius	MBS: 500 m, SBS: 50 m
Maximum transmit power	SBS: 24 dBm, UE: 23 dBm
Circuit power	30 dBm
Bandwidth	10 MHz
Intensity	SBS: $\lambda_s = 10$, UE: $\lambda_u = 2\lambda_s$
Thermal noise density and SI	-174 dBm/Hz, $\sigma_{\text{SI}}^2 = -110$ dB
DE parameter	$\alpha = 0.1$
Noise figure	SBS: 13 dB, UE: 9 dB
Path loss (in dB) SBS-to-SBS where d is in km	LOS: $98.4 + 20.9 \log_{10}(d)$ NLOS: $169.36 + 40 \log_{10}(d)$
Path loss (in dB) UE-to-SBS where d is in km	LOS: $103.8 + 20.9 \log_{10}(d)$ NLOS: $145.4 + 37.5 \log_{10}(d)$
Path loss (in dB) UE-to-UE where d is in km	LOS: $98.5 + 20 \log_{10}(d)$ NLOS: $175.78 + 40 \log_{10}(d)$

IV. NUMERICAL RESULTS AND DISCUSSIONS

The numerical simulation results obtained by using the distributed Algorithm 1 are presented in this section. A typical outdoor deployment scenario with a circular macro-cell area in the plane \mathbb{R}^2 is considered. One MBS located at the origin and ten randomly deployed SBSs, i.e., $B = 10$, whose locations follow an independent Poisson point process (PPP) $\Phi_s \in \mathbb{R}^2$ with intensity λ_s , are considered. We assume a total of two DL and two UL UEs within each SBS and they are randomly located according to the PPP $\Phi_u \in \mathbb{R}^2$ with intensity λ_u . Hence, the total number of UEs in the network is $K_D = K_U = 20$. The maximum transmission powers of SBSs and UEs are fixed and given by $P_{b,\text{max}}$ and P_{max} , respectively. The Rician fading model is considered to model the SI channel between the co-located transmitter-receiver antenna pair of an SBS with distribution $\mathcal{CN}(\sqrt{\sigma_{\text{SI}}^2 K/(1+K)} \mathbf{H}_{\text{SI}}, (\sigma_{\text{SI}}^2/(1+K)) \mathbf{I}_{M_R} \otimes \mathbf{I}_{M_T})$, where \mathbf{H}_{SI} is a deterministic matrix and K is the Rician factor with value 1, and σ_{SI}^2 is the SI variance. The rest of the channels in the system are assumed to be Rayleigh faded and the effect of the path and shadowing loss is already included in them. All other simulation parameters used are listed in Table I. We especially consider three system scenarios for comparison, which are referred to as: i) Setup-A: SBSs are powered by the grid source; ii) Setup-B: SBSs

are powered by a renewable energy source; and iii) Setup-C: SBSs are powered by a renewable energy source and consume energy for decoding UL UEs data. The number of bits waiting in the data buffer of each DL and UL UE are stored in vectors $Q^D = [6\ 7\ 4\ 5\ 3\ 2\ 2\ 2\ 2\ 3\ 1\ 1\ 2\ 2\ 2\ 3\ 2\ 2\ 3\ 7]$ and $Q^U = [3\ 7\ 3\ 5\ 7\ 3\ 2\ 3\ 1\ 3\ 3\ 3\ 3\ 1\ 2\ 2\ 2\ 2\ 3\ 2\ 1\ 1]$, respectively.

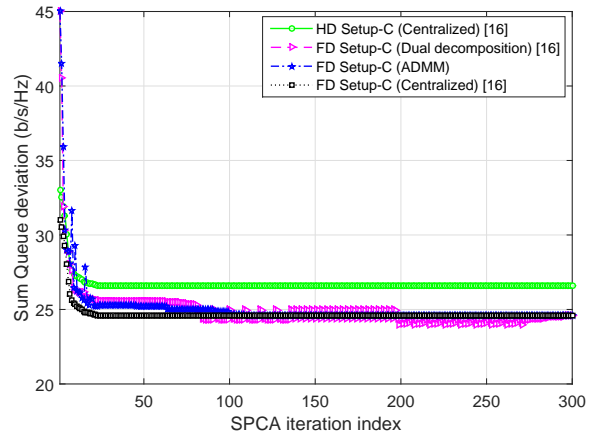


Fig. 2. Convergence of the proposed ADMM-based RAOFDS algorithm with respect to the SPCA iteration index.

We first compare the convergence of the proposed ADMM based distributed Algorithm 1 with the centralized and dual decomposition based distributed algorithms [16] in Fig. 2. The figure plots the total number of bits that remain in the network after each SPCA iteration step under the system Setup-C. It can be observed that the centralized algorithm converges faster than both ADMM and dual decomposition based distributed algorithms. However, among the distributed algorithms, the ADMM approach converges faster by taking approximately 200 iterations lesser than the dual decomposition approach, which takes 300 iterations. Note that all three algorithms converge to the same value of the queue deviation.

In Fig 2, the performance of the FD and HD SBSs is also compared. As expected, the FD SBSs achieve lower total queue deviation than the conventional HD SBSs. In next two examples, we only consider the performances of the FD SBSs for the presentation clarity.

Fig. 3 shows the sum rate performance achieved by the network with different values of the normalized energy arrival rates, i.e., $P_{b,H}/(P_b^{\text{cir}} + 5P_{b,\text{max}})$ at the SBSs under the Setup-B and Setup-C. For comparison, the sum rate of Setup-A is plotted; however, it is independent of the energy arrivals. In the low EH rate regime, for Setup-B, the sum rate is higher for UL as the SBS has lower energy availability for the DL UEs; hence, it produces low interference to the UL UEs. On the other hand, the DL transmissions achieve higher sum rate in the high EH rate regime. Consequently, the UL transmissions receive higher interference from the high power DL transmissions. This behavior is reversed for Setup-C, where the DL sum rates dominate in all EH rate regimes over the UL sum rates. The reason for this is that, in Setup-C, the SBS shares the harvested energy among the DL and UL UEs. Therefore, lower energy availability at the SBS limits the UL UEs from using lower transmit power that consequently introduces less interference into the DL transmissions.

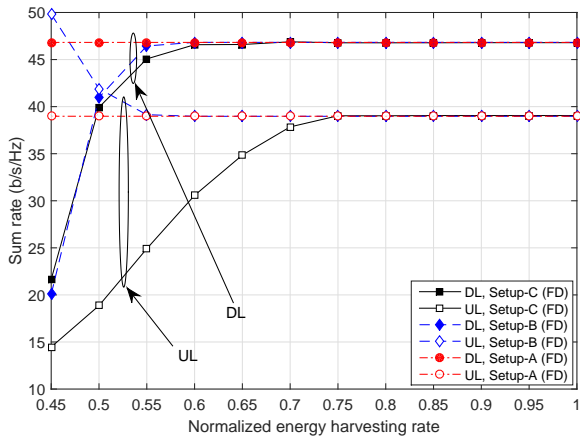


Fig. 3. DL and UL sum rate of the network with different normalized EH arrival rates at each SBS.

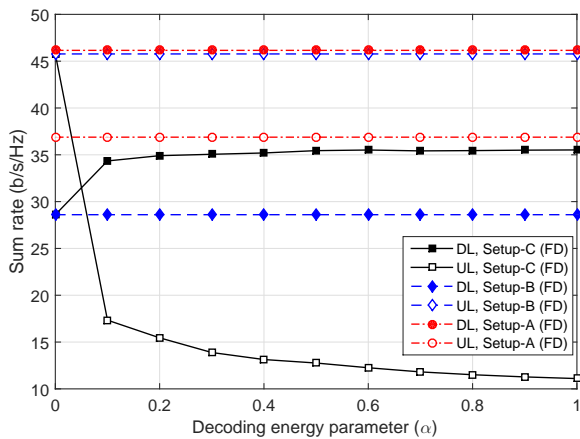


Fig. 4. DL and UL sum rate versus the DE parameters used by each SBS.

Fig. 4 show the sum rate achieved by the network under Setup-C with different values of the DE parameter. For comparison purposes, the figure also plots the sum rates achieved under the Setup-A and -B, which are independent of the DE parameter. Observe that the sum rate achieved by the UL UEs decreases with the increase in the portion of DE consumed at the SBS. This is because the UL UEs rates are now determined by the availability of the DE at the SBS. For instance, if the value of the DE parameter is small, the SBS allocates a small portion of the energy for the UL UEs decoding. This essentially means that the UL UEs cannot be decoded if transmitted at higher rate and UL UEs need to transmit with lower power. Consequently, a lower interference is experienced by the DL UEs, and thus, the sum rate improves as compared to Setup-B. High DE parameter values further restrict the UL UEs from transmitting at lower power, and hence, DL UEs experience low interference.

V. CONCLUSION

The performance of densely deployed FD small cells is studied at the network level. The SBSs are dependent on the renewable energy source for its transceiver operations. The UL UEs rate-dependent decoding energy is included in the total

energy consumption model at the SBSs. Hence, the energy harvested at the SBS must be optimally shared among the DL and UL UEs. A joint beamformer and power allocation design, which minimizes the UEs data buffer lengths, is proposed. Furthermore, the proposed optimization problem implicitly solves the problem of sub-carrier allocation and UEs scheduling. A sub-optimal and iterative SPCA-based approach is used to circumvent the non-convex nature of the problem. A fast-convergent algorithm based on the ADMM framework is proposed to solve the optimization problem distributively. Simulations are used to compare the performances of the proposed design under the practical energy consumption and casualty constraints with the case when the DE is not considered. Results show the performance gap and advocate the need for redesigning the beamformers and power allocations.

REFERENCES

- [1] N. Bhushan *et al.*, "Network densification: The dominant theme for wireless evolution into 5G," *IEEE Commun. Mag.*, vol. 52, no. 2, pp. 82–89, Feb. 2014.
- [2] X. Huang, T. Han, and N. Ansari, "On green-energy-powered cognitive radio networks," *IEEE Commun. Surveys Tut.*, vol. 17, no. 2, pp. 827–842, 2nd Quart. 2015.
- [3] P. He, L. Zhao, S. Zhou, and Z. Niu, "Recursive waterfilling for wireless links with energy harvesting transmitters," *IEEE Trans. Veh. Technol.*, vol. 63, no. 3, pp. 1232–1241, Mar. 2014.
- [4] I. Ahmed, A. Ikhlef, D. W. K. Ng, and R. Schober, "Power allocation for an energy harvesting transmitter with hybrid energy sources," *IEEE Trans. Wireless Commun.*, vol. 12, no. 12, pp. 6255–6267, Dec. 2013.
- [5] A. Arafa and S. Ulukus, "Optimal policies for wireless networks with energy harvesting transmitters and receivers: Effects of decoding costs," *IEEE J. Select. Areas Commun.*, vol. 33, no. 12, pp. 2611–2625, Dec. 2015.
- [6] A. Yadav, T. M. Nguyen, and W. Ajib, "Optimal energy management in hybrid energy small cell access points," *IEEE Trans. Commun.*, vol. 64, no. 12, pp. 5334–5348, Dec. 2016.
- [7] P. He and L. Zhao, "Optimal power allocation for maximum throughput of general MU-MIMO multiple access channels with mixed constraints," *IEEE Trans. Commun.*, vol. 64, no. 3, pp. 1042–1054, Mar. 2016.
- [8] —, "Non-commutative composite water-fillings for energy harvesting and smart power grid hybrid system with peak power constraints," *IEEE Trans. Veh. Technol.*, vol. 65, no. 4, pp. 2026–2037, Apr. 2016.
- [9] S. Hong *et al.*, "Applications of self-interference cancellation in 5G and beyond," *IEEE Commun. Mag.*, vol. 52, no. 2, pp. 114–121, Feb. 2014.
- [10] D. Bharadia, E. McMillin, and S. Katti, "Full duplex radios," *SIGCOMM Comput. Commun. Rev.*, vol. 43, no. 4, pp. 375–386, Aug. 2013.
- [11] D. Nguyen, L. N. Tran, P. Pirinen, and M. Latva-aho, "On the spectral efficiency of full-duplex small cell wireless systems," *IEEE Trans. Wireless Commun.*, vol. 13, no. 9, pp. 4896–4910, Sep. 2014.
- [12] S. Goyal, P. Liu, and S. S. Panwar, "User selection and power allocation in full duplex multi-cell networks," *IEEE Trans. Veh. Technol.*, vol. PP, no. 99, pp. 1–15, Jun. 2016.
- [13] S. Cui, A. Goldsmith, and A. Bahai, "Energy-efficiency of MIMO and cooperative MIMO techniques in sensor networks," *IEEE J. Select. Areas Commun.*, vol. 22, no. 6, pp. 1089–1098, Aug. 2004.
- [14] L. Chen *et al.*, "Green full-duplex self-backhaul and energy harvesting small cell networks with massive MIMO," *IEEE J. Select. Areas Commun.*, vol. 34, no. 12, pp. 3709–3724, Dec. 2016.
- [15] J. Rubio and A. Pascual-Iserte, "Energy-aware broadcast multiuser-MIMO precoder design with imperfect channel and battery knowledge," *IEEE Trans. Wireless Commun.*, vol. 13, no. 6, pp. 3137–3152, Jun. 2014.
- [16] A. Yadav, O. A. Dobre, and N. Ansari, "Energy and traffic aware full-duplex communications for 5G systems," *IEEE Access*, Mar. 2017 (to appear).
- [17] S. Boyd *et al.*, "Distributed optimization and statistical learning via the alternating direction method of multipliers," *Found. Trends Mach. Learn.*, vol. 3, no. 1, pp. 1–122, 2011.
- [18] A. Beck, A. Ben-Tal, and L. Tretushvili, "A sequential parametric convex approximation method with applications to nonconvex truss topology design problems," *J. Global Optim., Springer*, vol. 47, no. 1, pp. 29–51, May 2010.